

## Efficiency of Carbon Dioxide Storage and Enhanced Methane Recovery in a High Rank Coal

Hadi Mosleh, Mojgan; Sedighi, Majid; Vardon, Philip J.; Turner, Matthew

**DOI**

[10.1021/acs.energyfuels.7b02402](https://doi.org/10.1021/acs.energyfuels.7b02402)

**Publication date**

2017

**Document Version**

Accepted author manuscript

**Published in**

Energy & Fuels

**Citation (APA)**

Hadi Mosleh, M., Sedighi, M., Vardon, P. J., & Turner, M. (2017). Efficiency of Carbon Dioxide Storage and Enhanced Methane Recovery in a High Rank Coal. *Energy & Fuels*, 31(12), 13892-13900. <https://doi.org/10.1021/acs.energyfuels.7b02402>

**Important note**

To cite this publication, please use the final published version (if applicable). Please check the document version above.

**Copyright**

Other than for strictly personal use, it is not permitted to download, forward or distribute the text or part of it, without the consent of the author(s) and/or copyright holder(s), unless the work is under an open content license such as Creative Commons.

**Takedown policy**

Please contact us and provide details if you believe this document breaches copyrights. We will remove access to the work immediately and investigate your claim.

1  
2  
3  
4 **1 Efficiency of carbon dioxide storage and enhanced methane**  
5 **2 recovery in a high rank coal**  
6  
7  
8  
9

4 Mojgan Hadi Mosleh<sup>1,2\*</sup>, Majid Sedighi<sup>1,2</sup>, Philip J. Vardon<sup>1,3</sup>, and Matthew Turner<sup>1,4</sup>  
5

6 <sup>1</sup> Geoenvironmental Research Centre, School of Engineering, Cardiff University, The Queen's  
7 Buildings, Newport Road, Cardiff, CF24 3AA, UK

8 <sup>2</sup> School of Mechanical, Aerospace and Civil Engineering, The University of Manchester,  
9 Manchester, M13 9PL, UK

10 <sup>3</sup> Section of Geo-Engineering, Faculty of Civil Engineering and Geosciences, Delft University of  
11 Technology, 2600 GA, Delft, The Netherlands

12 <sup>4</sup> IHS Global Limited, Enterprise House, Cirencester Road, Tetbury, GL8 8RX, UK  
13

14 \* Corresponding author (email: [mojgan.hadimosleh@manchester.ac.uk](mailto:mojgan.hadimosleh@manchester.ac.uk))  
15  
16  
17  
18  
19  
20  
21  
22  
23  
24  
25  
26  
27  
28  
29  
30  
31  
32  
33  
34  
35  
36  
37  
38  
39  
40  
41  
42  
43  
44  
45  
46  
47  
48  
49  
50  
51  
52  
53  
54  
55  
56  
57  
58  
59  
60

1  
2  
3  
4 **16 Abstract**

5  
6 17 High affinity and adsorption capacity of coal to carbon dioxide provides alternative approach for  
7  
8 18 the enhanced recovery of methane from unminable coalfields (CO<sub>2</sub>-ECBM) by which a potential  
9  
10 19 solution for long-term CO<sub>2</sub> sequestration in deep geological formations can also be achieved.  
11  
12 20 However, due to chemo-mechanical effects induced by the interactions between CO<sub>2</sub> and coal, the  
13  
14 21 effective methane production and carbon dioxide storage can be degraded which has caused  
15  
16 22 uncertainties about the techno-economic feasibility of the CO<sub>2</sub>-ECBM process. This study presents  
17  
18 23 an experimental investigation that aims to address key knowledge gaps related to the efficiency of  
19  
20 24 CO<sub>2</sub> storage and CH<sub>4</sub> recovery in high rank coals for which comprehensive experimental data set  
21  
22 25 and analysis are largely missing. Competitive displacements of CH<sub>4</sub> with N<sub>2</sub> or CO<sub>2</sub> in an  
23  
24 26 anthracite coal sample from South Wales coalfield have been studied, based on a series of core  
25  
26 27 flooding experiments.

27  
28 28 The results show that the N<sub>2</sub> breakthrough time (the time at which 1% of the total gas injected was  
29  
30 29 recovered) was almost spontaneous whereas a considerably delayed breakthrough time was  
31  
32 30 observed for the case of CO<sub>2</sub>-ECBM experiment. In addition it was observed that for the CO<sub>2</sub>-  
33  
34 31 ECBM experiment, the ratios of CH<sub>4</sub> recovery with respect to the total amount of gas injected and  
35  
36 32 gas stored were higher by factors of 10 and 2.4, respectively. The results also show that 90% of the  
37  
38 33 total N<sub>2</sub> injected was produced in the outflow gas, whereas for the case of the CO<sub>2</sub> experiment, only  
39  
40 34 63% of the total injected CO<sub>2</sub> was produced. Presence of high amount of N<sub>2</sub> in the outflow may  
41  
42 35 lead to additional challenges in order to separate N<sub>2</sub> from CH<sub>4</sub> and thus affects the efficiency of the  
43  
44 36 N<sub>2</sub>-ECBM method. Under the conditions of the experiments, the total CH<sub>4</sub> displacement ratio and  
45  
46 37 breakthrough for the case CO<sub>2</sub>-ECBM were found to be more favorable compared to those obtained  
47  
48 38 from N<sub>2</sub>-ECBM. This study provides new insights into the efficiency of CO<sub>2</sub>-ECBM process and  
49  
50 39 offers a comprehensive experimental data set that can be used for testing the accuracy of predictive  
51  
52 40 models.

1  
2  
3  
4  
5  
6  
7  
8  
9  
10  
11  
12  
13  
14  
15  
16  
17  
18  
19  
20  
21  
22  
23  
24  
25  
26  
27  
28  
29  
30  
31  
32  
33  
34  
35  
36  
37  
38  
39  
40  
41  
42  
43  
44  
45  
46  
47  
48  
49  
50  
51  
52  
53  
54  
55  
56  
57  
58  
59  
60

41 **Keywords:** *CO<sub>2</sub> sequestration, enhanced coalbed methane recovery (ECBM), anthracite coal, core*  
42 *flooding, gas permeability, gas sorption, South Wales coalfield.*  
43

## 1. Introduction

The process of coalbed methane (CBM) production from unminable coal fields usually involves the pressure depletion in the coal reservoir by pumping out the naturally existing formation water. However, the pressure depletion only allows a limited amount of in-place-gas ( $\text{CH}_4$ ) to be produced because the methane is adsorbed on the coal even at low pressures (White et al., 2005). As a result, approximately 30 to 70% of the in-place-gas in coal cannot be recovered using the conventional pressure depletion method (Puri and Yee, 1990). Enhanced coalbed methane (ECBM) recovery is a process by which  $\text{N}_2$  or  $\text{CO}_2$  (or a mixture of both) is injected into the coal seam to enhance the recovery of coalbed methane (White et al., 2005). In  $\text{N}_2$ -ECBM,  $\text{N}_2$  first displaces the free  $\text{CH}_4$  from the seam and reduces the partial pressure of methane in the reservoir that enables further methane in the adsorbed phase (in coal matrix) to be released (Shi and Durucan, 2005). However, rapid breakthrough of  $\text{N}_2$  during the production of methane has been reported to be the major issue in the field projects (Perera and Ranjith, 2015). Alternatively,  $\text{CO}_2$  has been suggested to enhance the coalbed methane recovery ( $\text{CO}_2$ -ECBM) due to the higher affinity of coal to adsorb carbon dioxide compared to methane that may result in larger amount of coalbed methane production. In addition, the potential long term sequestration of  $\text{CO}_2$  in deep unminable coal seams during the process of  $\text{CO}_2$ -ECBM is an advantage over the  $\text{N}_2$ -ECBM process (Shi and Durucan, 2005). Permeability evolution in coal as the result of changes in effective stress and sorption-induced swelling and shrinkage during ECBM process has been extensively studied by researchers, through laboratory investigation and numerical modeling, *e.g.* Feng et al. (2017), Hadi Mosleh et al. (2017), Liu and Harpalani (2013), Ma et al. (2011). Experimental studies show that coal can exhibit shrinkage or swelling during interaction with different gas species, *e.g.* Mazumder et al. (2006), Mazzotti et al. (2009), Hadi Mosleh (2014). Therefore, the uptake or release of  $\text{CO}_2$  and  $\text{CH}_4$  is a combination of adsorption/desorption

1  
2  
3  
4 68 processes and coal swelling/shrinkage that can affect the permeability of the coal, resulting in the  
5  
6 69 overall rate and efficiency of methane recovery and carbon dioxide storage.  
7

8 70 Observations from limited pilot tests of carbon sequestration in coal seams that have been reported  
9  
10 71 in the literature (Japan, Poland and China) indicate the reduction in the injectivity of carbon dioxide  
11  
12 72 as the result of reduction in coal permeability induced by swelling (Reeves and Oudinot, 2005;  
13  
14 73 Yamaguchi et al. 2006; van Bergen et al. 2006). However, the outcomes of the field tests reported  
15  
16 74 have largely remained inconclusive (Pan and Connell, 2012). A limited number of lab-scale  
17  
18 75 experimental studies have also been reported on processes related to enhanced coalbed methane  
19  
20 76 recovery nitrogen and carbon dioxide, *e.g.* van Hemert et al. (2012), Wang et al. (2010), Mazumder  
21  
22 77 and Wolf (2008), Yu et al. (2008). The experimental approach adopted in majority of these studies  
23  
24 78 is based on core flooding test in which a core sample of coal is first saturated with CH<sub>4</sub> and then N<sub>2</sub>  
25  
26 79 or CO<sub>2</sub> (or a mixture if gas) is injected into the sample. The composition of the outflow gas is  
27  
28 80 monitored during the test to evaluate the breakthrough time of the injected gas, displacement of  
29  
30 81 gases and the rate of gas storage/recovery. Wang et al. (2010) carried out a series of gas storage and  
31  
32 82 recovery experiments on highly volatile bituminous coal and showed that for the example  
33  
34 83 considered, the amount of the adsorbed CO<sub>2</sub> was two orders of magnitude larger as compared to the  
35  
36 84 amount of desorbed CH<sub>4</sub>. Yu et al. (2008) has reported gas storage and recovery experiments on  
37  
38 85 coal samples originated from Qinshui basin in China. The results show that initially the CO<sub>2</sub>  
39  
40 86 fraction in the outflow gas was very small compared to the CH<sub>4</sub> and the initial CH<sub>4</sub> displacement  
41  
42 87 with CO<sub>2</sub> was not associated with the CO<sub>2</sub> release. They have also shown that with an increase of  
43  
44 88 the volume of replaced CH<sub>4</sub>, the discharge capacity of CO<sub>2</sub> has slowly increased.  
45

46 89 Compared to the extensive experimental investigations carried out on adsorption/desorption  
47  
48 90 characteristics and permeability properties of coal to gas species, the laboratory scale experimental  
49  
50 91 studies on the process of N<sub>2</sub>-ECBM and CO<sub>2</sub>-ECBM are very limited and comparative assessment  
51  
52 92 of the efficiency of enhanced methane recovery by N<sub>2</sub> and CO<sub>2</sub> is still lacking. In the last decade  
53  
54 93 several conceptual models have been developed to account for the flow of gas in coal and fractured  
55  
56  
57  
58  
59  
60

1  
2  
3  
4 94 rock (e.g. Shi and Durucan, 2003; Salimzadeh and Khalili, 2015; Hosking, 2014). These models are  
5  
6 95 usually based on mechanistic approaches that require appropriate constitutive relationships (e.g.  
7  
8 96 gas permeability model) and experimental data for testing. Data sets generated from laboratory  
9  
10 97 scale experiments on N<sub>2</sub>-ECBM and CO<sub>2</sub>-ECBM are critical bench marks for testing such  
11  
12 98 numerical models that can be used for simulation and design of the process at field scale.  
13  
14 99 However, the experimental studies that contain adequate material properties and provide  
15  
16 100 constitutive relationships for numerical modeling are scarce, especially for high rank coals, *i.e.*  
17  
18 101 anthracite. In this work, we aim to address i) gaps in knowledge related to the response of a high  
19  
20 102 rank coal to gas injection, displacement and storage during ECBM process, and ii) the lack of  
21  
22 103 adequate and comprehensive experimental dataset required for testing the predictive models. In this  
23  
24 104 paper, an experimental investigation on the process of N<sub>2</sub>-ECBM and CO<sub>2</sub>-ECBM in a high rank  
25  
26 105 coal from South Wales coalfield is presented and comparative assessment of the efficiency based  
27  
28 106 on gas recovery and storage for both N<sub>2</sub>-ECBM and CO<sub>2</sub>-ECBM is discussed. Core flooding  
29  
30 107 experiments have been conducted in which N<sub>2</sub> and CO<sub>2</sub> were injected into the CH<sub>4</sub>-saturated coal  
31  
32 108 sample to evaluate the competitive displacement of CH<sub>4</sub> with N<sub>2</sub> and CO<sub>2</sub> under simulated  
33  
34 109 underground conditions. The displacement process, gas breakthrough, and recovery ratios are also  
35  
36 110 discussed.

## 111 **2. Material and methods**

112 The anthracite coal sample used in this work was obtained from the Six Feet coal seam, at the  
113 Unity coal mine located in South Wales, UK (Hadi Mosleh et al., 2017). Blocks of coal with  
114 dimensions of approximately 0.5×0.5×0.5m were collected from the depth of approximately 550m.  
115 Prior to core flooding experiments, a series of coal characterisation tests including the Proximate  
116 and Ultimate Analyses (BS 1016-104 and BS 1016-106) were conducted on crushed samples in  
117 order to determine key properties of moisture content, ash content, and volatile matter as well as  
118 elemental composition such as sulphur and carbon contents. Table 1 presents a summary of the  
119 physical and chemical properties of the coal used.

## 120 **2.1. Preparation of core samples**

121 The core sample used was drilled from a large block of coal using a diamond core drill bit with  
122 70mm internal diameter. The core sample was then cut into the required length using a diamond  
123 saw. Special care was taken during the coring and cutting processes to minimise breakage or  
124 damage to the coal structure. Any small breakage especially around the edges could potentially  
125 damage or puncture the rubber membrane during triaxial core flooding tests and under the high  
126 confining pressures and therefore had to be removed. In order to prevent breakage of the coal  
127 samples under high stress conditions, the ends of the specimens were ground and made parallel to  
128 each other using a fine sand paper. This allowed a uniform distribution of the axial stresses to both  
129 ends of the sample. In order to remove any residual moisture, the core sample was then air-dried  
130 for 24hr before it was placed in the triaxial cell for the tests.

## 131 **2.2. Triaxial core flooding setup**

132 Triaxial core flooding setup was designed and developed by Hadi Mosleh (2014). The experimental  
133 setup comprises i) a high pressure triaxial core flooding system, ii) a pressure control system, iii) a  
134 temperature control system, and iv) an ancillary system including gas supply and analysing units. A  
135 schematic diagram of the developed laboratory facility is presented in Figure 1 (Hadi Mosleh et al.,  
136 2017).

137 The core sample sits within a 1.5mm thick silicone rubber sleeve and the gas passes through a  
138 porous plate at the bottom of the sample, then it leaves the cell through a similar arrangement at the  
139 top after having passed through the test core. A Mass Flow Meter capable of measuring high flow  
140 rates up to  $17 \times 10^{-6} \text{m}^3/\text{s}$  (1L/min) is connected to the outlet which is capable of working under both  
141 subcritical and supercritical conditions, with pressures up to 20MPa.

142 The pressure control system includes a pressure/volume controller to control the confining pressure  
143 and a high pressure regulator with a needle valve to control the gas pore pressure. Two 32MPa in-  
144 line pore pressure transducers were selected to measure the inlet and the outlet gas pressures. The  
145 confining system consists of a 32MPa pressure/volume controller with a  $2 \times 10^{-4} \text{m}^3$  (200mL) oil



1  
2  
3  
4 146 reservoir. Volume changes can be measured and displayed to  $1 \times 10^{-9} \text{m}^3$  (0.001mL). The confining  
5  
6 147 pressure is provided by silicone oil 350 (Polydimethylsiloxane) and a hydraulic pump. The  
7  
8 148 composition of the outflow gases was determined using an Emerson X-Stream general purpose gas  
9  
10 149 analyser (standard 19"/3HU version) with the optimum gas flow rate of  $1.7 \times 10^{-5} \text{m}^3/\text{s}$  (1L/min) and  
11  
12 150  $\pm 0.01\%$  accuracy of Full Range Output (FRO). More details of the design and development of the  
13  
14 151 laboratory setup can be found in Hadi Mosleh et al. (2017).  
15

### 17 152 **2.3. Experimental procedure**

18  
19 153 The core sample of 70mm diameter and 100mm length was carefully wrapped with a thick PTFE  
20  
21 154 tape before being placed in the silicone rubber sleeve. The displacement transducers, two axial and  
22  
23 155 one radial, and three thermocouples were then attached to the sample. The top cap was placed on  
24  
25 156 the base pedestal and the cell was filled with the silicone oil. The temperature of the system was  
26  
27 157 adjusted to  $25^\circ\text{C}$  (the corresponding temperature of the depth at which the sample was taken), using  
28  
29 158 four heating elements attached to the cell's body and a programmable controller. The temperature  
30  
31 159 was kept constant throughout the test. A confining pressure of 1MPa was applied and the sample  
32  
33 160 was subjected to vacuum for 24 hours to remove the residual moisture and gases from the pore  
34  
35 161 space. Prior to each core flooding test, the core sample was saturated with the chosen gas.  
36

37 162 The steady-state method has been used to estimate permeability of the coal sample (Carles et al.,  
38  
39 163 2007). For the initial permeability measurements, the confining pressure was maintained at the  
40  
41 164 desired pressure and increased stepwise. Once the steady-state flow rate was achieved at each step,  
42  
43 165 the differential gas pressures and gas flow rates were recorded. The permeability of the coal sample  
44  
45 166 was calculated using Darcy's law (Carman, 1956), given as:

$$k_g = \frac{2Q_0\mu_g LP_0}{A(P_{up}^2 - P_{down}^2)} \quad (1)$$

48  
49  
50  
51  
52 167 where,  $k_g$  is the gas permeability coefficient ( $\text{m}^2$ ),  $Q_0$  is the volumetric rate of flow ( $\text{m}^3/\text{s}$ ),  $\mu_g$  is the  
53  
54 168 viscosity of the gas (Pa.s),  $L$  is the sample length (m) and  $P_0$  refers to the reference pressure (Pa)  
55  
56  
57  
58  
59  
60

1  
2  
3  
4 169 which in this study was atmospheric pressure, *i.e.*  $1 \times 10^5$  Pa.  $A$  is the cross-sectional area of the  
5  
6 170 sample ( $m^2$ ),  $P_{up}$  is the upstream gas pressure (Pa), and  $P_{down}$  is the downstream gas pressure (Pa).  
7  
8 171 The viscosity of gases ( $\mu_g$ ) was calculated as function of temperature, using the Sutherland formula  
9  
10 172 (Smits and Dussauge, 2006).

11  
12 173 The experimental tests carried out based on the steps summarised in Figure 2:

#### 14 15 174 **Stage 1: Flow characterisation of the coal sample**

16  
17 175 Since helium is a non-adsorptive/non-reactive gas it was used to characterise the coal sample for its  
18  
19 176 intrinsic permeability and to investigate the mechanical effect of stresses on permeability of coal  
20  
21 177 during gas injection and depletion processes. The intrinsic permeability to helium has been used as  
22  
23 178 a key material property to compare gas flow behaviour of the coal sample used in this study with  
24  
25 179 those from previous studies, *i.e.* Hadi Mosleh (2014), and also to evaluate the changes in  
26  
27 180 permeability of the same coal sample with respect to gas species. The permeability of the coal  
28  
29 181 sample to helium was estimated for a range of gas injection pressures (up to 5.5MPa) and at several  
30  
31 182 confining pressures (up to 6MPa). In order to evaluate the effects of confining pressure on the gas  
32  
33 183 flow properties of the coal sample, the confining pressure was first increased stepwise up to 6MPa  
34  
35 184 while gas injection pressure was kept constant at 3.5MPa. To assess the effect of pore pressure  
36  
37 185 changes on gas flow and permeability of the coal sample, gas pressure was increased gradually to  
38  
39 186 5.5MPa while the confining pressure was kept constant (6MPa). The coal sample was then  
40  
41 187 subjected to vacuum for 24 hours and saturated with  $CH_4$  at 5MPa injection pressure and 6MPa  
42  
43 188 confining pressure. The permeability of the coal to  $CH_4$  was measured by performing a  $CH_4$   
44  
45 189 flooding experiment under a range of gas injection pressures from 3.5 to 5.5MPa.

#### 46 47 48 190 **Stage 2: $N_2$ - and $CO_2$ -ECBM experiments**

49  
50 191 The coal sample was re-saturated with  $CH_4$  at 5MPa injection pressure and 6MPa confining  
51  
52 192 pressure.  $N_2$  gas was then injected into the  $CH_4$ -saturated at 5MPa injection pressure while the  
53  
54 193 downstream valve was at atmospheric pressure, *i.e.* 0.1MPa. The composition of the outflow gas  
55  
56  
57  
58  
59  
60

1  
2  
3  
4 194 was analysed during the experiment using the gas analyser. After the N<sub>2</sub>-ECBM experiment, the  
5  
6 195 residual gas was removed from the sample by applying vacuum. The sample was purged with CH<sub>4</sub>  
7  
8 196 While the composition of outflow gas was monitored using the gas analyser until no residual N<sub>2</sub>  
9  
10 197 was present in the outflow. The sample was then re-saturated with CH<sub>4</sub>, and CO<sub>2</sub> subsequently was  
11  
12 198 injected at 5 MPa. The confining pressure was kept constant throughout at 6MPa. The composition  
13  
14 199 of the outflow gas was monitored continuously and the test was continued until CH<sub>4</sub> was mostly  
15  
16 200 displaced with CO<sub>2</sub>. Figure 3 presents a schematic diagram of the experimental conditions applied  
17  
18 201 for the N<sub>2</sub>- and CO<sub>2</sub>-ECBM experiments.

## 202 **3. Results and discussions**

### 203 **3.1. Helium flooding experiment**

204 For low permeability coals, the flow behaviour is highly dependent on the effective stress (Huy et  
25  
26 205 al., 2010). For incompressible fluid such as water, the effective stress is defined as the difference  
27  
28 206 between the confining pressure and linear mean gas pressure across the sample (Harpalani and  
29  
30 207 Chen, 1997):

$$31 \quad \sigma_{eff} = P_c - \frac{P_{up} + P_{down}}{2} \quad (2)$$

32  
33  
34  
35  
36  
37 208 where,  $\sigma_{eff}$  is the effective stress and  $P_c$  is the confining pressure.

38  
39  
40 209 Since gas is compressible, its bulk density varies greatly which in turn has a significant effect on  
41  
42 210 gas transport within the porous medium. Therefore unlike incompressible fluids, variation of gas  
43  
44 211 pore pressure across sample length is not expected to be linear. In this study, the analytical solution  
45  
46 212 presented by Wu et al. (1998) has been used to estimate the changes in gas pore pressure across the  
47  
48 213 sample at steady-state flow conditions:

$$49 \quad P(x) = -b + \sqrt{b^2 + P_L^2 + 2bP_L + 2q_m \mu(L-x) / k_\infty \beta} \quad (3)$$

50  
51  
52  
53 214 where,  $P(x)$  is the gas pressure (Pa) at linear distance  $x$  (m),  $b$  is the Klinkenberg coefficient,  $P_L$  is  
54  
55 215 the gas pressure at outlet boundaries of linear flow systems (Pa),  $q_m$  is the gas mass injection or

1  
2  
3  
4 216 pumping flux ( $\text{kg/s.m}^2$ ),  $L$  is the length of linear flow systems or thickness of unsaturated zone (m),  
5  
6 217  $k_{co}$  is the absolute permeability ( $\text{m}^2$ ), and  $\beta$  is the compressibility factor;  $\mu$  viscosity (Pa.s).

7  
8 218 The length of the sample was divided into 7 sections of 0.02m long, and for each section the  
9  
10 219 average pore pressure was estimated using Eq. (3). In general, the average pore pressure within the  
11  
12 220 coal sample obtained from Eq. (3) was found to be approximately 26-28% higher than average pore  
13  
14 221 pressure obtained from linear approximation method. The mean gas pore pressure obtained from  
15  
16 222 Eq. (3) was then used to estimate the effective stress, using Eq. (2).

17  
18 223 The variations of permeability of the coal sample to helium with effective stress are presented in  
19  
20 224 Figure 4a. Based on the results, the permeability of the coal sample ranges between 0.15 and  
21  
22 225  $0.45 \times 10^{-15} \text{m}^2$  over the range of applied pressures and confining stresses applied. Variations in  
23  
24 226 confining pressure and gas pore pressure showed slightly different effects on permeability  
25  
26 227 evolution of the coal sample, however the overall trends of permeability behaviour as a result of  
27  
28 228 changes in confining pressure and gas pore pressure were similar, *i.e.* the coal permeability to  
29  
30 229 helium was reduced with increase in effective stress. These results are consistent with the results of  
31  
32 230 another series of core flooding experiments performed by Hadi Mosleh (2014) on a similar coal  
33  
34 231 sample (sister sample) obtained from same block of coal (Figure 4b). Coal permeability variations  
35  
36 232 with effective stress can be attributed to the expansion or closure of the internal fractures and  
37  
38 233 microfractures (Vishal et al., 2013). Non-linear evolution of coal permeability to gases with  
39  
40 234 effective stress has been reported by other researchers (*e.g.* Feng et al., 2016; Mitra et al., 2012).

### 41 42 43 235 **3.2. CH<sub>4</sub> flooding experiment**

44  
45 236 The CH<sub>4</sub> core flooding experiment was performed to evaluate the initial permeability of the coal  
46  
47 237 sample to CH<sub>4</sub> before introducing CO<sub>2</sub> during the gas storage and recovery experiments and its  
48  
49 238 consequent swelling effect on gas flow properties of coal. The results of the coal permeability to  
50  
51 239 CH<sub>4</sub> versus effective stress are presented in Figure 5. The coal permeability to CH<sub>4</sub> was found to  
52  
53 240 vary between  $0.03 \times 10^{-15} \text{m}^2$  and  $0.14 \times 10^{-15} \text{m}^2$  under the applied stresses. In general, the  
54  
55 241 permeability of the coal sample to CH<sub>4</sub> was found to be one order of magnitude lower than that to

1  
2  
3  
4 242 helium which can be mainly related to their differences in molecular size. The effect of gas  
5  
6 243 sorption-induced permeability evolution of coal should also be taken into account when  
7  
8 244 interpreting such results. The range of permeability evolution of coal reported in the literature as  
9  
10 245 the result of CH<sub>4</sub> interaction with coal matrix varies greatly. For instance, Harpalani and Mitra  
11  
12 246 (2010) have reported a CH<sub>4</sub> permeability reduction of approximately 25% compared to the original  
13  
14 247 value, whereas in a study conducted by Milewska-Duda et al. (2000), the effect of CH<sub>4</sub> on coal  
15  
16 248 matrix swelling and permeability reduction was found to be negligible, compared to highly reactive  
17  
18 249 gases such as CO<sub>2</sub>.

19  
20 250 Once the evaluation of the initial properties of the coal sample was completed, the coal sample was  
21  
22 251 re-saturated with CH<sub>4</sub> at injection pressure of 5MPa and confining pressure of 6MPa.

### 252 **3.3. N<sub>2</sub> - ECBM recovery**

253 The results of the gas displacement process during the N<sub>2</sub>-ECBM experiment are presented in  
254 Figure 6. The results present the variation of the gas composition in the outflow with time. It can be  
255 observed that an early breakthrough of the injected N<sub>2</sub> has occurred shortly after the injection  
256 process was started. The definition of the breakthrough time of the injected gas varies in the  
257 literature. A common definition for the breakthrough in work related to gas storage and recovery  
258 processes has been considered here which is described as the time at which 1% of the total gas  
259 injected is recovered (van Hemert et al., 2012; Mazumder and Wolf, 2008; Ross, 2007). In this  
260 case, the breakthrough time was less than 100s.

261 The breakthrough time reported in the literature might vary greatly ranging from several minutes to  
262 several days depending on the coal type, sample size, permeability, gas injection pressure, injection  
263 rate and effective stresses, *e.g.* Connell et al. (2011), Shi et al. (2008), Yu et al. (2008). The early  
264 breakthrough observed in the N<sub>2</sub>-ECBM experiment and relatively fast displacements of CH<sub>4</sub> are  
265 primarily related to the displacement of the free gas existing within the coal cleats/microfractures  
266 rather than the free gas in the coal matrix. This is related to the experimental conditions in which a  
267 relatively high injection pressure has been applied under low effective stress on the sample.

1  
2  
3  
4 268 The results presented in Figure 6 show that within the first half an hour of the experiment, more  
5  
6 269 than 95% of the production gas consisted of N<sub>2</sub>. Rapid changes in N<sub>2</sub> and CH<sub>4</sub> fractions at this stage  
7  
8 270 of the experiment can be attributed to the displacement of the free or weakly adsorbed CH<sub>4</sub>  
9  
10 271 molecules with N<sub>2</sub>. Therefore, the dominant gas exchange process at this stage was the differences  
11  
12 272 in the partial pressures of N<sub>2</sub> and CH<sub>4</sub> within the coal cleats and microfractures. As the experiment  
13  
14 273 continued, the rate of changes in the fraction of CH<sub>4</sub> in the production gas became very slow and  
15  
16 274 remained steady and continuous. This can be related to the slow diffusion of N<sub>2</sub> and CH<sub>4</sub> in the coal  
17  
18 275 matrix (Cui et al., 2004), which is the dominant gas exchange process at this stage of the  
19  
20 276 experiment. As a result, the diffusion of N<sub>2</sub> into the coal matrix gradually reduces the partial  
21  
22 277 pressure of CH<sub>4</sub> in the coal matrix and eventually leads to CH<sub>4</sub> desorption.

#### 24 278 **3.4. CO<sub>2</sub> - ECBM recovery**

26 279 The experimental results of the gas displacement process during the CO<sub>2</sub>-ECBM experiment are  
27  
28 280 presented in Figure 7 which shows the variations of gas composition in the production gas with  
29  
30 281 time as a result of CH<sub>4</sub> displacement with CO<sub>2</sub>. The small spikes on the graph are related to the  
31  
32 282 minor fluctuations in the injection pressure generated as a result of simultaneous operation of the  
33  
34 283 gas booster.

36 284 From the results presented, it is apparent that the breakthrough time of CO<sub>2</sub> is two times slower  
37  
38 285 than the N<sub>2</sub>-ECBM experiment that can be attributed to a combination of gas diffusion process in  
39  
40 286 the coal and the effects of coal matrix swelling induced by the CO<sub>2</sub> adsorption. Although, the  
41  
42 287 volumetric deformation has not been directly measured in the experiments presented here,  
43  
44 288 reduction in the mass flow rate of outflow gas during the CO<sub>2</sub>-ECBM experiment demonstrate the  
45  
46 289 significance of the effect of coal swelling on the flow process. The mass flow rates recorded at  
47  
48 290 downstream of the sample reduced from 14g/h to 1g/h during the course of CO<sub>2</sub>-ECBM experiment  
49  
50 291 (more than 5 hours), whereas for the case of N<sub>2</sub>-ECBM experiment, the recorded mass-flow rates  
51  
52 292 remained relatively steady throughout the experiment, *i.e.* 28-34g/h.

1  
2  
3  
4 293 With its relatively smaller kinetic diameter, CO<sub>2</sub> molecules can penetrate into the micro-pores of  
5  
6 294 coal which are inaccessible or less accessible to CH<sub>4</sub> and N<sub>2</sub> molecules that have larger kinetic  
7  
8 295 diameters. This can result in one or two orders of magnitude higher diffusivity of CO<sub>2</sub> in the coal  
9  
10 296 matrix compared with N<sub>2</sub> and CH<sub>4</sub> (Cui et al., 2004). Hence, the higher diffusion of CO<sub>2</sub> than that  
11  
12 297 for CH<sub>4</sub> and N<sub>2</sub> may limit its breakthrough in the production gas through faster diffusion into the  
13  
14 298 coal matrix. Moreover, the effect of the coal swelling induced by CO<sub>2</sub> adsorption can also result in  
15  
16 299 slower rate of gas flow in the cleat and consequently increases the time of the breakthrough.

17  
18 300 The results of the gas storage and recovery experiments show that, the overall rate of CO<sub>2</sub>  
19  
20 301 displacement with CH<sub>4</sub> is much slower compared to case for N<sub>2</sub>. For the N<sub>2</sub> experiment, more than  
21  
22 302 95% of CH<sub>4</sub> has been displaced within less than 30 minutes, whereas for the case of CO<sub>2</sub>  
23  
24 303 experiment, the fraction of displaced CH<sub>4</sub> has almost reached 90% after 3 hours of continuous CO<sub>2</sub>  
25  
26 304 injection. As stated earlier, higher diffusion rate of CO<sub>2</sub> and the effect of sorption-induced swelling  
27  
28 305 on coal matrix during the CO<sub>2</sub>-ECBM process can together govern the slower gas displacement  
29  
30 306 rates observed. Whereas, in the N<sub>2</sub>-ECBM process, the slower rate of N<sub>2</sub> diffusion into the coal  
31  
32 307 matrix leads to relatively higher partial pressure of N<sub>2</sub> gas within the coal cleats and therefore faster  
33  
34 308 gas displacement rate and N<sub>2</sub> breakthrough is observed.

### 309 **3.5. Gas storage and recovery in coal**

38  
39 310 Based on the experimental data of gas flow rates at upstream and downstream obtained from two  
40  
41 311 mass flow meters, and the composition of the outflow gas obtained from gas analyser, the upstream  
42  
43 312 and downstream mass flow rates were estimated and converted to mole per second (mol/s). The  
44  
45 313 cumulative amounts of gas injected, recovered and stored in the coal sample were then calculated  
46  
47 314 for each experiment. It should be mentioned that the gas storage here implies the total amount of  
48  
49 315 gas adsorbed to the coal matrix as well as the free gas stored in cleats/microfractures and matrix  
50  
51 316 pore volume. Figures 8 and 9 present the cumulative amounts of gas injected, recovered and stored  
52  
53 317 in the coal sample during N<sub>2</sub>- and CO<sub>2</sub>-ECBM experiments, respectively.

1  
2  
3  
4 318 The results presented in Figures 8 and 9 show that for the same duration of the experiment and  
5  
6 319 under similar experimental conditions, the total amount of injected  $N_2$  was 11 times higher than  
7  
8 320 that for  $CO_2$  injection. In addition, the results show that 90% of the total injected  $N_2$  was in the  
9  
10 321 production gas, whereas in the case of the  $CO_2$  experiment, only 63% of the total injected  $CO_2$  was  
11  
12 322 in the production gas. Therefore 36% of the injected  $CO_2$  has been retained within the coal sample.

13  
14 323 In another study conducted by Hadi Mosleh (2014), the maximum adsorption capacity of the same  
15  
16 324 coal to  $CO_2$  was estimated 1.21mol/kg. By assuming the total amount of stored  $CO_2$  during  $CO_2$ -  
17  
18 325 ECBM experiment as adsorbed gas, it can be postulated that only 20% of the adsorption capacity of  
19  
20 326 coal sample to  $CO_2$  was utilised. This can be related to several factors:

- 21  
22 327 • Effect of gas diffusion rate: the gas adsorption isotherms were measured on powdered coal  
23  
24 328 samples and over 24 to 48 hours, when the equilibrium state was observed (Hadi Mosleh, 2014),  
25  
26 329 whereas the experiments of this study have been conducted on intact 70mm core samples, and  
27  
28 330 over shorter durations (~4hr). Therefore, much longer time was needed for the gas to diffuse  
29  
30 331 into the coal matrix and to achieve equilibrium state.
- 31  
32 332 • Effect of coal swelling: coal swells when it comes into contact with  $CO_2$ , this resulted in  
33  
34 333 reduction of coal permeability under confined conditions and therefore a reduction in the  
35  
36 334 accessibility of the coal matrix to more  $CO_2$  gas.
- 37  
38 335 • Effect of effective stress on coal permeability: in gas adsorption measurements by Hadi Mosleh  
39  
40 336 (2014), powdered coal was placed in a high pressure cell without confining pressure applied to  
41  
42 337 coal sample. Whereas in this study, the results of helium and  $CH_4$  flooding experiments have  
43  
44 338 shown that permeability of the coal decreases as effective stress increases. This is related to  
45  
46 339 compression of fractures and microfractures and therefore reduction in accessibility of coal  
47  
48 340 matrix to gas.

51  
52 341 **3.6. Efficiency of  $CH_4$  recovery**  
53  
54  
55  
56  
57  
58  
59  
60



1  
2  
3  
4 342 Figure 10 shows the cumulative amounts of CH<sub>4</sub> recovered during the N<sub>2</sub>-ECBM and CO<sub>2</sub>-ECBM  
5  
6 343 experiments. From the results, it may be suggested that the total amounts of CH<sub>4</sub> recovered in N<sub>2</sub>-  
7  
8 344 and CO<sub>2</sub>-ECBM experiments are almost equal (0.187mol and 183mol, respectively) and therefore  
9  
10 345 both methods can be equally effective in terms of CH<sub>4</sub> recovery. However the rate of CH<sub>4</sub> recovery,  
11  
12 346 which is an important factor affecting the success of ECBM application, should be taken into  
13  
14 347 account when interpreting such results. The results presented in Figure 10 show that the rate of CH<sub>4</sub>  
15  
16 348 recovery for the case of N<sub>2</sub> injection was significantly higher at the early stages of the experiment  
17  
18 349 and reduced considerably for much of the experiment's duration; whereas for the case of CO<sub>2</sub>  
19  
20 350 injection, the rate of CH<sub>4</sub> was found to be more or less steady throughout the experiment. Similar  
21  
22 351 observations have been reported by Yu et al. (2008) based on the core flooding experiments  
23  
24 352 conducted on coal samples from Qinshui basin in North China.

25  
26 353

27  
28 354 In addition, the efficiency of CH<sub>4</sub> recovery from coal can be related to other factors including: i)  
29  
30 355 the amount of gas required for the injection, ii) the fraction of injected gas in the production gas  
31  
32 356 which needs to be separated from CH<sub>4</sub>, and iii) the amount of gas that can be stored in coal which  
33  
34 357 is particularly important for the case of CO<sub>2</sub> sequestration process. Figures 11 and 12 present the  
35  
36 358 ratio of CH<sub>4</sub> recovery with respect to the amount of gas injected and stored, respectively, during  
37  
38 359 both N<sub>2</sub> and CO<sub>2</sub> experiments.

39  
40  
41 360 The results of CH<sub>4</sub> recovery versus injected gas (Figure 11) indicate that the CO<sub>2</sub> injection lead to a  
42  
43 361 higher ratio of CH<sub>4</sub> recovery throughout the experiment (up to 10 times higher than that obtained  
44  
45 362 by N<sub>2</sub> injection). This is mainly related to the higher amounts of N<sub>2</sub> injected under similar  
46  
47 363 experimental conditions, *i.e.* gas injection pressure and confining pressure. The amount of the CH<sub>4</sub>  
48  
49 364 recovery for both experiments decreased sharply in the first hour of the experiments. The rate of  
50  
51 365 CH<sub>4</sub> recovery, however, remained almost steady for the N<sub>2</sub> experiment after the first hour, whereas  
52  
53 366 for the CO<sub>2</sub> experiment, it decreased gradually over time. This behaviour can be attributed to the  
54  
55 367 effect of coal matrix swelling on gas permeability and flow as described previously.

1  
2  
3  
4 368 The results of CH<sub>4</sub> recovery versus stored gas (Figure 12) also show that storage of CO<sub>2</sub> lead to  
5  
6 369 higher ratio of CH<sub>4</sub> recovery (on average 2.4 times higher than that obtained by N<sub>2</sub> injection). In  
7  
8 370 other words, for every mole of CO<sub>2</sub> stored in the coal sample 1.2mol of CH<sub>4</sub> was recovered. Higher  
9  
10 371 ratios have also been reported in the literature, *e.g.* a ratio of 2 to 1 (Tsotsis et al., 2004) which can  
11  
12 372 be related to the differences in coal type (different sorption capacities and gas flow and mechanical  
13  
14 373 properties) and the experimental conditions.

#### 16 374 **4. Conclusions**

17  
18  
19 375 The results of gas storage and recovery from a series of experiments conducted on the CH<sub>4</sub>  
20  
21 376 saturated coal sample were presented on a high rank coal from South Wales coalfield. N<sub>2</sub> and CO<sub>2</sub>  
22  
23 377 were injected at the upstream of the sample and composition of outflow gas was monitored. The  
24  
25 378 results of both experiments were assessed and compared in terms of breakthrough time, gas  
26  
27 379 displacement rate, and efficiency of gas storage and recovery.

28  
29  
30 380 The results showed that the N<sub>2</sub> breakthrough time was almost spontaneous whereas for the case of  
31  
32 381 CO<sub>2</sub>, the breakthrough time was delayed by a factor of two. Similarly, the gas displacement rate  
33  
34 382 observed in both experiments varied greatly which was mostly related to differences between  
35  
36 383 diffusivity of N<sub>2</sub> and CO<sub>2</sub> as well as higher affinity of the coal to CO<sub>2</sub>. The latter effect also  
37  
38 384 resulted in storage of 36% of injected CO<sub>2</sub> in coal. The results of CH<sub>4</sub> recovery showed that with  
39  
40 385 respect to both injected and stored gas, the ratios of CH<sub>4</sub> recovered during CO<sub>2</sub> experiment were  
41  
42 386 higher than those for N<sub>2</sub> experiment.

43  
44 387 This study has shown that early N<sub>2</sub> breakthrough and higher rate of N<sub>2</sub> production may lead to  
45  
46 388 additional challenges in order to separate N<sub>2</sub> from CH<sub>4</sub> and thus affects the efficiency of the N<sub>2</sub>-  
47  
48 389 ECBM method. For the case of CO<sub>2</sub>, the total CH<sub>4</sub> recovery, displacement ratio, breakthrough and  
49  
50 390 CO<sub>2</sub> storage are more favourable. In general, the displacement ratio, CO<sub>2</sub> breakthrough time and  
51  
52 391 CO<sub>2</sub> storage are important parameters affecting the success of carbon sequestration application and

1  
2  
3  
4 392 the results of this study provide new insights into the efficiency of gas recovery and storage in  
5  
6 393 anthracite coal using carbon dioxide and under the experimental conditions applied.  
7

#### 8 9 394 **Acknowledgements**

10  
11 395 The financial support received from the Welsh-European Funding Office as part of the  
12  
13 396 Geoenvironmental Research Centre's SEREN project is gratefully acknowledged. The authors  
14  
15 397 would like to thank Dr Snehasis Tripathy for his support. We also would like to thank GDS  
16  
17 398 Instruments for their contribution for construction and commissioning of laboratory equipment.  
18  
19 399 Technical support from the technicians and staff of the Engineering Workshop at Cardiff  
20  
21 400 University is also gratefully acknowledged.  
22  
23

#### 24 401 **References**

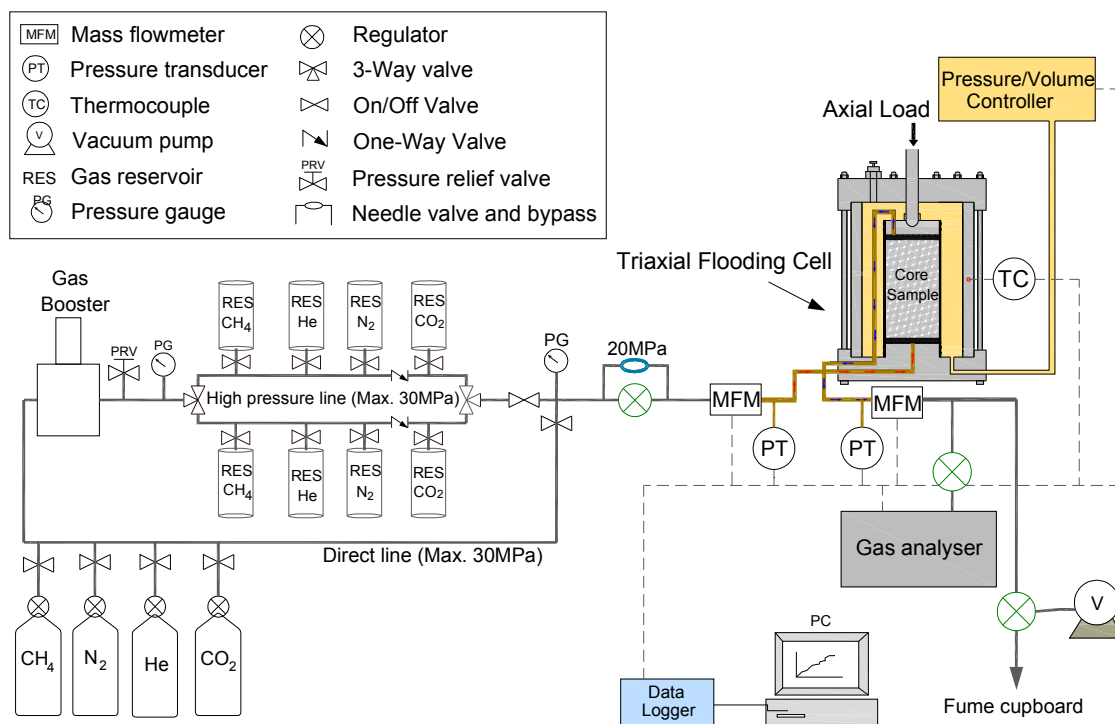
- 25  
26  
27 402 Carles, P., Egermann, P., Lenormand, R. and Lombard, J. 2007. Low permeability measurements  
28 403 using steady-state and transient methods. *The International Symposium of the Society of Core*  
29 404 *Analysts*, Calgary, Canada. 10-14 September 2007.
- 30  
31 405 Carman, P.C. 1956. *Flow of gases through porous media*. London: Butterworths.
- 32  
33 406 Connell, L.D., Sander, R., Pan, Z., Camilleri, M. and Heryanto, D. 2011. History matching of  
34 407 enhanced coal bed methane laboratory core flood tests. *International Journal of Coal Geology*,  
35 408 87(2), 128-138.
- 36  
37 409 Cui, X., Bustin, R.M. and Dipple, G. 2004. Selective transport of CO<sub>2</sub>, CH<sub>4</sub> and N<sub>2</sub> in coals:  
38 410 insights from modeling of experimental gas adsorption data. *Fuel*, 83(3), pp. 293-303.
- 39  
40 411 Durucan, S. and Edwards, J.S. 1986. The effects of stress and fracturing on permeability of coal.  
41 412 *Mining Science and Technology*, 3(3), pp. 205-216.
- 42  
43 413 Feng, R., Harpalani, S., and Pandey R. 2016. Laboratory measurement of stress-dependent coal  
44 414 permeability using pulse-decay technique and flow modeling with gas depletion. *Fuel*, 177, pp. 76-  
45 415 86.
- 46  
47 416 Feng, R., Harpalani, S., and Liu, J. 2017. Optimized pressure pulse-decay method for laboratory  
48 417 estimation of gas permeability of sorptive reservoirs: Part 2 - Experimental study. *Fuel*, (191), pp.  
49 418 565-573.
- 50  
51 419 Hadi Mosleh, M. 2014. An experimental investigation of flow and reaction processes during gas  
52 420 storage and displacement in coal. *PhD Thesis*, Cardiff University.
- 53  
54 421 Hadi Mosleh, M., Turner, M., Sedighi, M., and Vardon, P.J. 2017. High Pressure Gas Flow,  
55 422 Storage and Displacement in Fractured Rock-Experimental Setup Development and Application,  
56 423 *Review of Scientific Instruments*, 88(1), 015108:1-14.

- 1  
2  
3  
4 424 Harpalani, S. and Chen, G. 1997. Influence of gas production induced volumetric strain on  
5 425 permeability of coal. *Geotechnical and Geological Engineering*, 15(4), pp. 303-25.
- 6  
7 426 Hosking, L. 2014. Reactive transport modelling of high pressure gas flow in coal. *PhD Thesis*,  
8 427 Cardiff University.
- 9  
10 428 Huy, P.Q., Sasaki, K., Sugai, Y. and Ichikawa, S. 2010. Carbon dioxide gas permeability of coal  
11 429 core samples and estimation of fracture aperture width. *International Journal of Coal Geology*,  
12 430 83(1), pp. 1-10.
- 13  
14 431 Karacan, C.Ö. 2003. Heterogeneous sorption and swelling in a confined and stressed coal during  
15 432 CO<sub>2</sub> injection. *Energy and Fuels*, 17(6), pp. 1595-1608.
- 16  
17 433 Liu, S., and Harpalani, S. 2013. Permeability prediction of coalbed methane reservoirs during  
18 434 primary depletion. *International Journal of Coal Geology*, 113, pp. 1-10.
- 19  
20 435 Ma, Q., Harpalani, S., and Liu, S. 2011. A simplified permeability model for coalbed methane  
21 436 reservoirs based on matchstick strain and constant volume theory. *International Journal of Coal*  
22 437 *Geology*, 85(1), pp. 43-48.
- 23  
24 438 Mazumder, S., Karnik, A. and Wolf, K.H. 2006. Swelling of coal in response to CO<sub>2</sub> sequestration  
25 439 for ECBM and its effect on fracture permeability. *SPE Journal*, 11(3), pp. 390-398.
- 26  
27 440 Mazumder, S. and Wolf, K. 2008. Differential swelling and permability change of coal in response  
28 441 to CO<sub>2</sub> injection for ECBM. *International Journal of Coal Geology*, 74(2), pp. 123-138.
- 29  
30 442 Milewska-Duda, J., Duda, J., Nodzenski, A. and Lakatos, J. 2000. Absorption and adsorption of  
31 443 methane and carbon dioxide in hard coal and active carbon. *Langmuir*, 16(12), pp. 5458-5466.
- 32  
33 444 Mitra, A., Harpalani, S., and Liu, S. 2012. Laboratory measurement and modeling of coal  
34 445 permeability with continued methane production: Part 1 – Laboratory results. *Fuel*, 94, pp. 110-  
35 446 116.
- 36  
37 447 Onur Balan, H. 2008. Modeling the effects of variable coal properties on methane production  
38 448 during enhanced coalbed methane recovery. MSc Thesis, Middle East Technical University.
- 39  
40 449 Pan, Z. and Connell, L.D. 2012. Modelling permeability for coal reservoirs: A review of analytical  
41 450 models and testing data. *International Journal of Coal Geology*, 92(1), pp. 1-44.
- 42  
43 451 Perera, M.S.A. and Ranjith, P.G. 2015. Enhanced Coal Bed Methane Recovery: Using Injection of  
44 452 Nitrogen and Carbon Dioxide Mixture. Handbook of Clean Energy Systems, John Wiley & Sons,  
45 453 Ltd.
- 46  
47 454 Puri, R., and Yee, D. 1990. Enhanced coalbed methane recovery. Society of Petroleum  
48 455 Engineering, 65<sup>th</sup> Annual Techn. Conf., New Orleans (LA). Paper 20732, pp. 193-202.
- 49  
50 456 Reeves, S., and Oudinot, A. 2005. The Allison unit CO<sub>2</sub>-ECBM pilot - a reservoir and economic  
51 457 analysis. *Proceedings of the 2005 International Coalbed Methane Symposium*, Tuscaloosa,  
52 458 Alabama. Paper 0522.
- 53  
54 459 Ross, H.E. 2007. Carbon dioxide sequestration and enhanced coalbed methane recovery in  
55 460 unmineable coalbeds of the Powder River Basin, Wyoming. PhD Thesis, Stanford University.

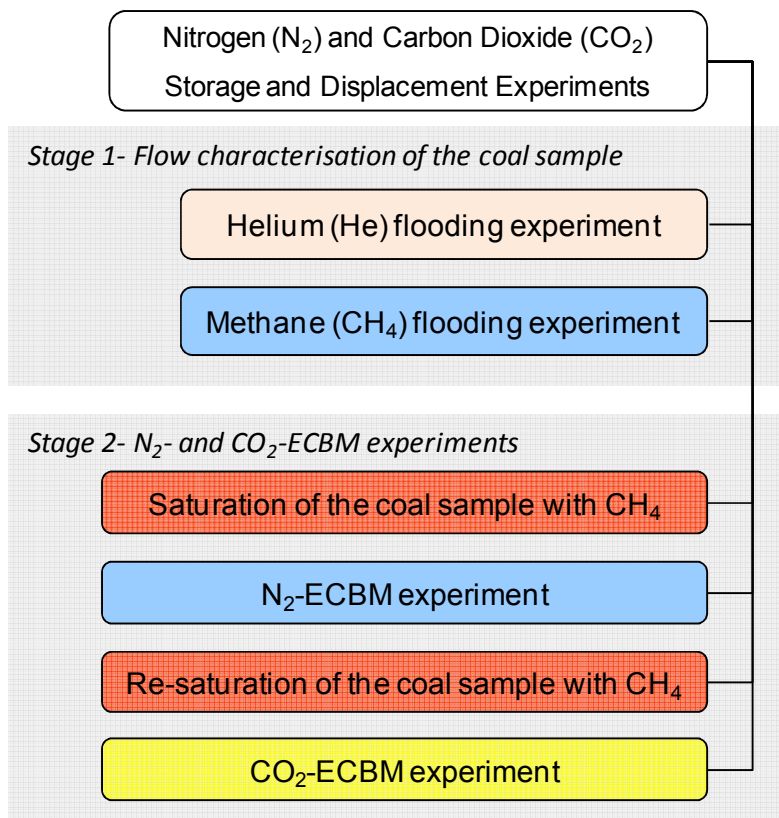
- 1  
2  
3  
4 461 Salimzadeh, S., and Khalili, N. 2015. Three-Dimensional Numerical Model for Double-Porosity  
5 462 Media with Two Miscible Fluids Including Geomechanical Response. *International Journal of*  
6 463 *Geomechanics*, 16(3).
- 7  
8 464 Shi, J-Q., and Durucan, S. 2003. A bidisperse pore diffusion model for methane displacement  
9 465 desorption in coal by CO<sub>2</sub> injection. *Fuel*, 82(10), pp. 1219-1229.
- 10  
11 466 Shi, J-Q., and Durucan, S. 2005. CO<sub>2</sub> storage in deep unminable coal seams. *Oil & Gas Science*  
12 467 *and Technology-Rev.IFP*, 60(3), pp. 547-558.
- 13  
14 468 Shi, J-Q., Mazumder, S., Wolf, K. and Durucan, S. 2008. Competitive methane desorption by  
15 469 supercritical CO<sub>2</sub> injection in coal. *Transport in Porous Media*, 75(1), pp. 35-54.
- 16  
17 470 Smits, A.J. and Dussauge, J.P. 2006. *Turbulent Shear Layers in Supersonic Flow*. 2nd ed. New  
18 471 York: American Institute of Physics.
- 19  
20 472 Somerton, W.H., Soylemezoglu, I.M. and Dudley, R.C. 1975. Effect of stress on permeability of  
21 473 coal. *International Journal of Rock Mechanics and Mining Sciences & Geomechanics*, 12(5-6), pp.  
22 474 129-45.
- 23  
24 475 Tsotsis, T.T., Patel, H., Najafi, B.F., Racherla, D., Knackstedt, M.A. and Sahimi, M. 2004.  
25 476 Overview of laboratory and modelling studies of carbon dioxide sequestration in coal beds.  
26 477 *Industrial and Engineering Chemistry Research*, 43(12), pp. 2887-2901.
- 27  
28 478 Van Bergen, F., Pagnier, H., Krzystolik, P., 2006. Field experiment of enhanced coalbed methane-  
29 479 CO<sub>2</sub> in the upper Silesian basin of Poland. *Environmental Geosciences* 13(3),201–224.
- 30  
31 480 van Hemert, P., Wolf, K. and Rudolph, E.S.J. 2012. Output gas stream composition from methane  
32 481 saturated coal during injection of nitrogen, carbon dioxide, a nitrogen-carbon dioxide mixture and a  
33 482 hydrogen-carbon dioxide mixture. *International Journal of Coal Geology*, 89(1), pp. 108-113.
- 34  
35 483 Vishal, V., Ranjith, P.G. and Singh, T.N. 2013. CO<sub>2</sub> permeability of Indian bituminous coals:  
36 484 Implications for carbon sequestration. *International Journal of Coal Geology*, 105(1), pp. 36-47.
- 37  
38 485 White, C.M., Smith, D.H., Jones, K.L., Goodman, A.L., Jikich, S.A., LaCount, R.B., DuBose, S.B.,  
39 486 Ozdemir, E., Morsi, B.I. and Schroeder, K.T. 2005. Sequestration of carbon dioxide in coal with  
40 487 enhanced coalbed methane recovery- A review. *Energy and Fuel*, 19(3), p. 659-724.
- 41  
42 488 Wu, Y-S., Pruess, K. and Persoff, P. (1998). Gas flow in porous media with Klinkenberg effects.  
43 489 *Transport in Porous Media*, 32, 117-137.
- 44  
45 490 Yamaguchi, S., Ohga, K., Fujioka, M., 2006. Field experiment of Japan sequestration in coal seams  
46 491 project (JCOP). *Proceedings of the 8<sup>th</sup> CO<sub>2</sub> International Conference on Greenhouse Gas Control*  
47 492 *Technologies*, Trondheim, Norway, June 19C22, 2006.
- 48  
49 493 Yu, H., Zhou, L., Guo, W., Cheng, J. and Hu, Q. 2008. Predictions of the adsorption equilibrium of  
50 494 methane/carbon dioxide binary gas on coals using Langmuir and ideal adsorbed solution theory  
51 495 under feed gas conditions. *International Journal of Coal Geology*, 73(2), pp. 115-129.

**Table 1.** Physical and chemical properties of the coal sample.

Moisture (wt%)	1.2	Carbon (%)	86.4
Sample diameter ( <i>mm</i> )	70	Volatile matter (%)	9.7
Sample length ( <i>mm</i> )	120	Fixed carbon (%)	84.4
Bulk density (kg/m <sup>3</sup> )	1398	Sulphur (%)	0.8
Porosity (-)	0.05	Ash (%)	4.9



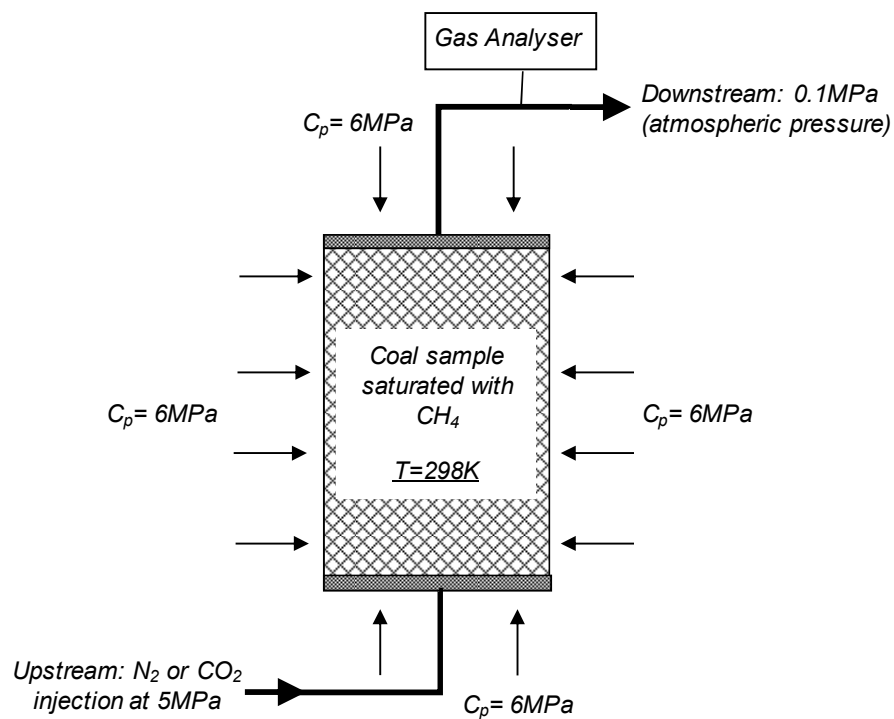
27 **Figure 1.** A schematic diagram of the developed laboratory facility (Hadi Mosleh et al., 2017).



30  
31  
32  
33  
34  
35  
36  
37  
38  
39  
40  
41  
42  
43  
44  
45  
46  
47  
48  
49  
50  
51  
52  
53  
54  
55  
56  
57  
58  
59  
60

**Figure 2.** The order of experimental studies carried out.





27 **Figure 3.** Schematic diagram of the experimental conditions applied for the  $\text{N}_2$  and  $\text{CO}_2$  ECBM  
28 experiments,  $C_p$  is the confining pressure.  
29  
30  
31  
32  
33  
34  
35  
36  
37  
38  
39  
40  
41  
42  
43  
44  
45  
46  
47  
48  
49  
50  
51  
52  
53  
54  
55  
56  
57  
58  
59  
60

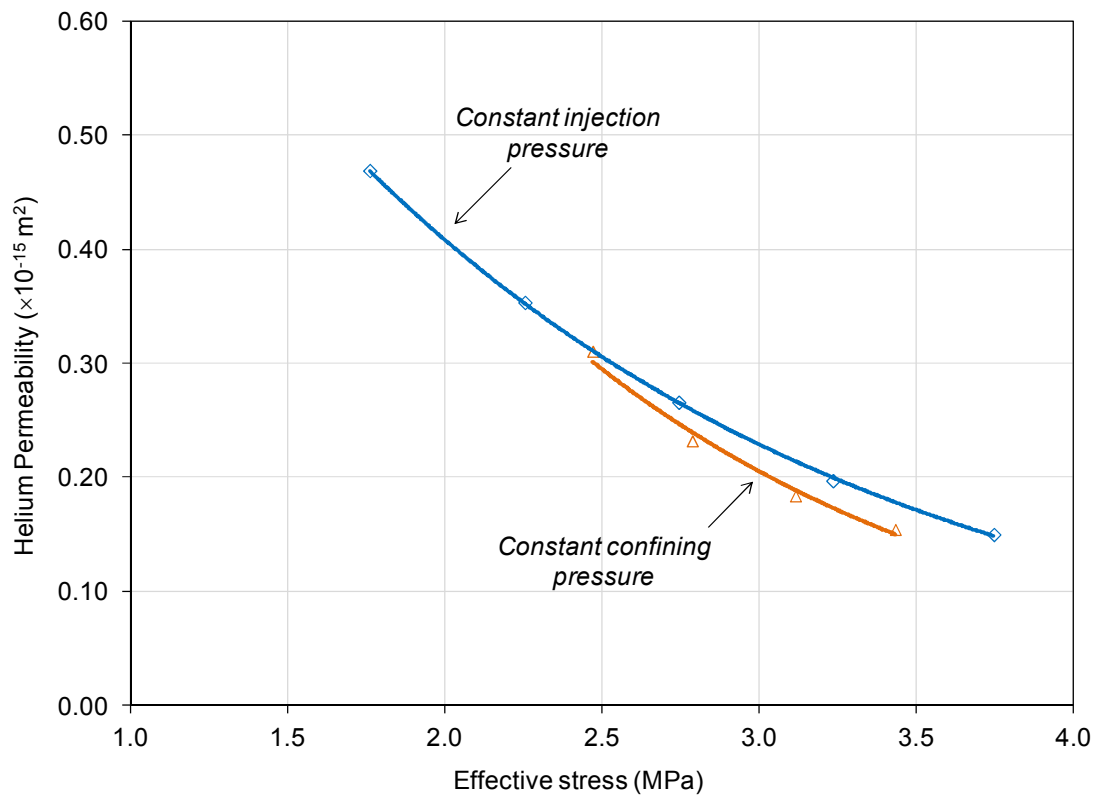


**Figure 4a.** Variations of the coal permeability to helium with effective stress under constant injection pressure and constant confining pressure.

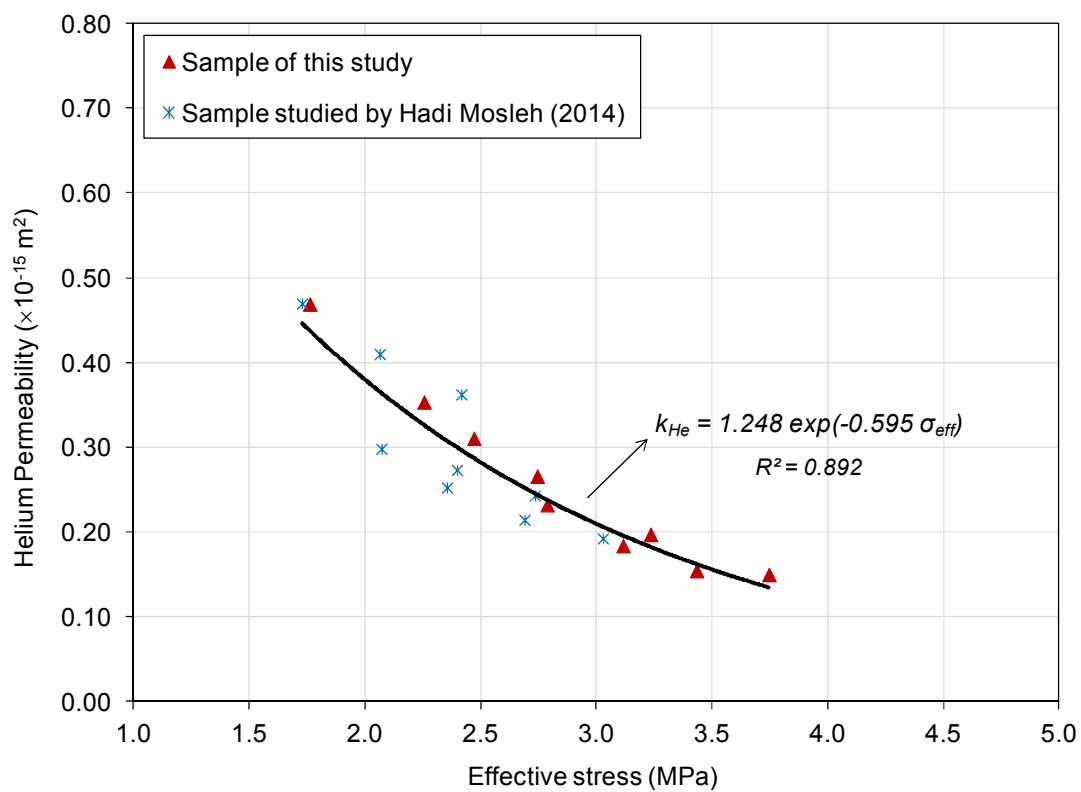


**Figure 4b.** Variation of coal permeability to helium with effective stress for the sample of this study and a sister sample obtained from same block of coal (Hadi Mosleh, 2014).

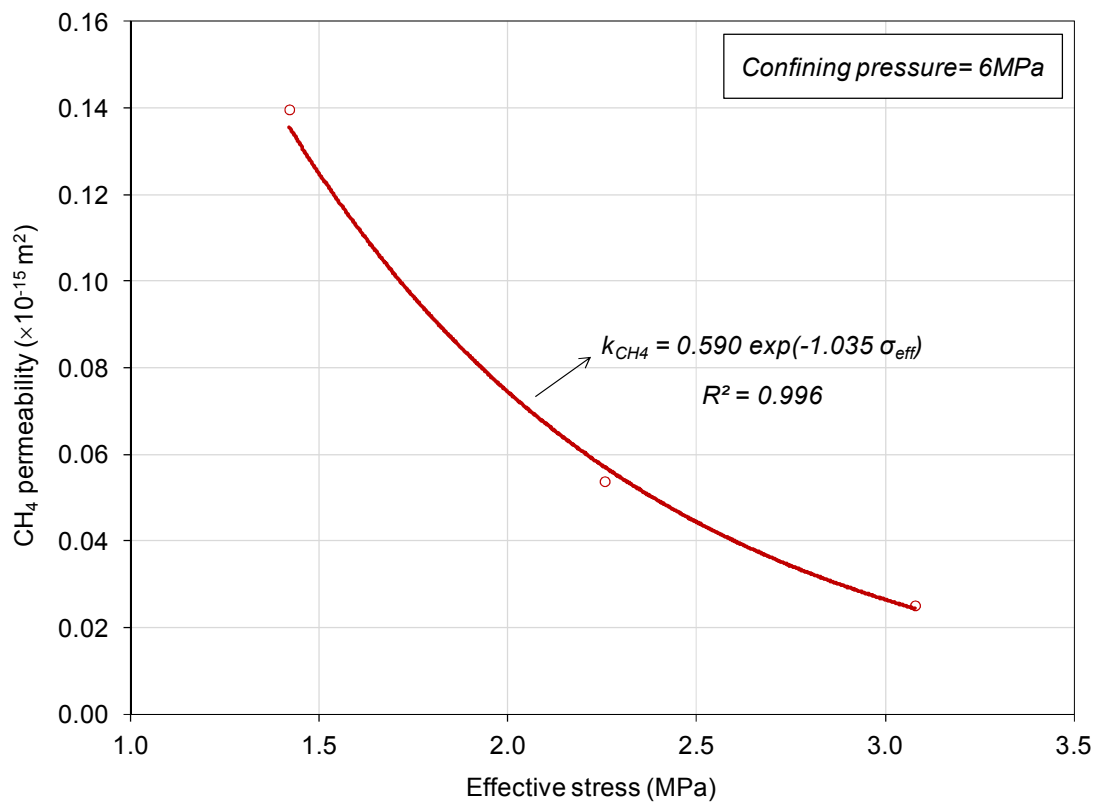


**Figure 5.** The relationship between permeability of the coal sample to CH<sub>4</sub> and effective stress.

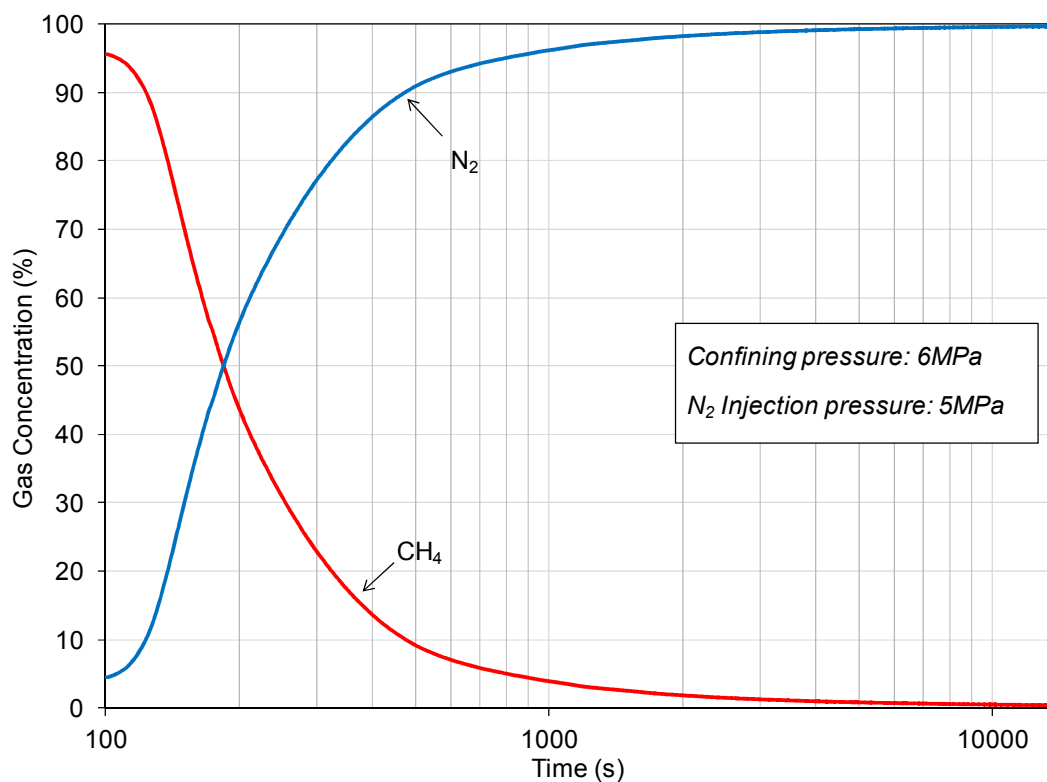
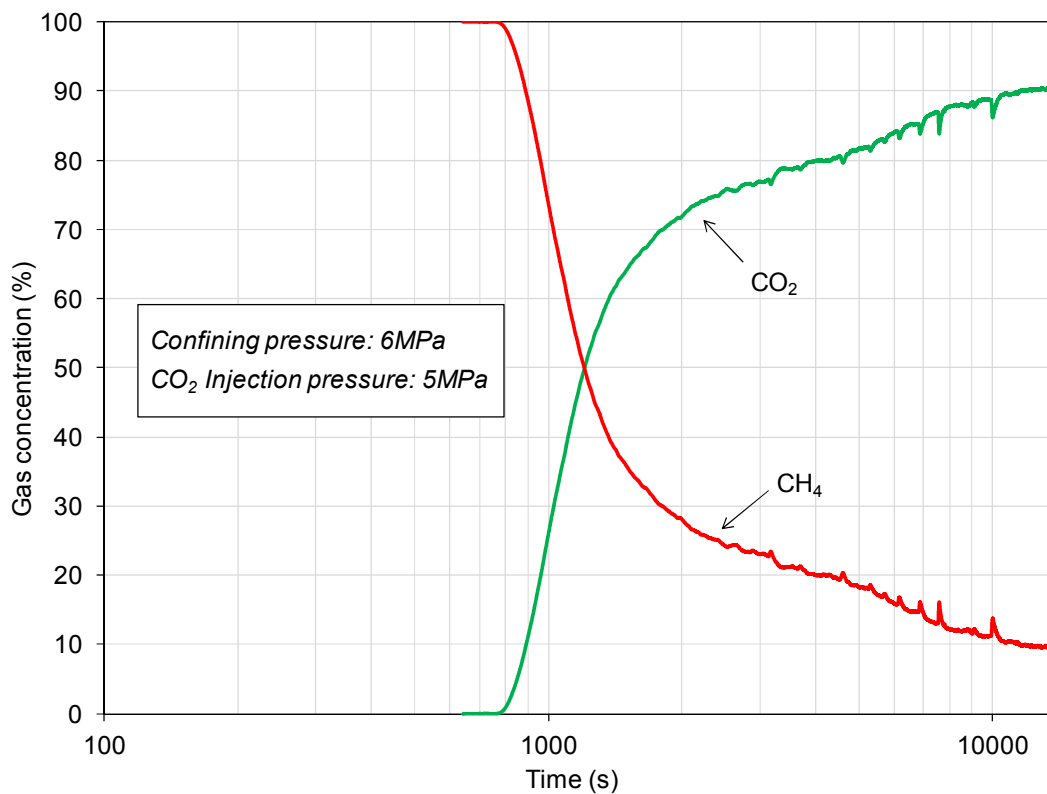
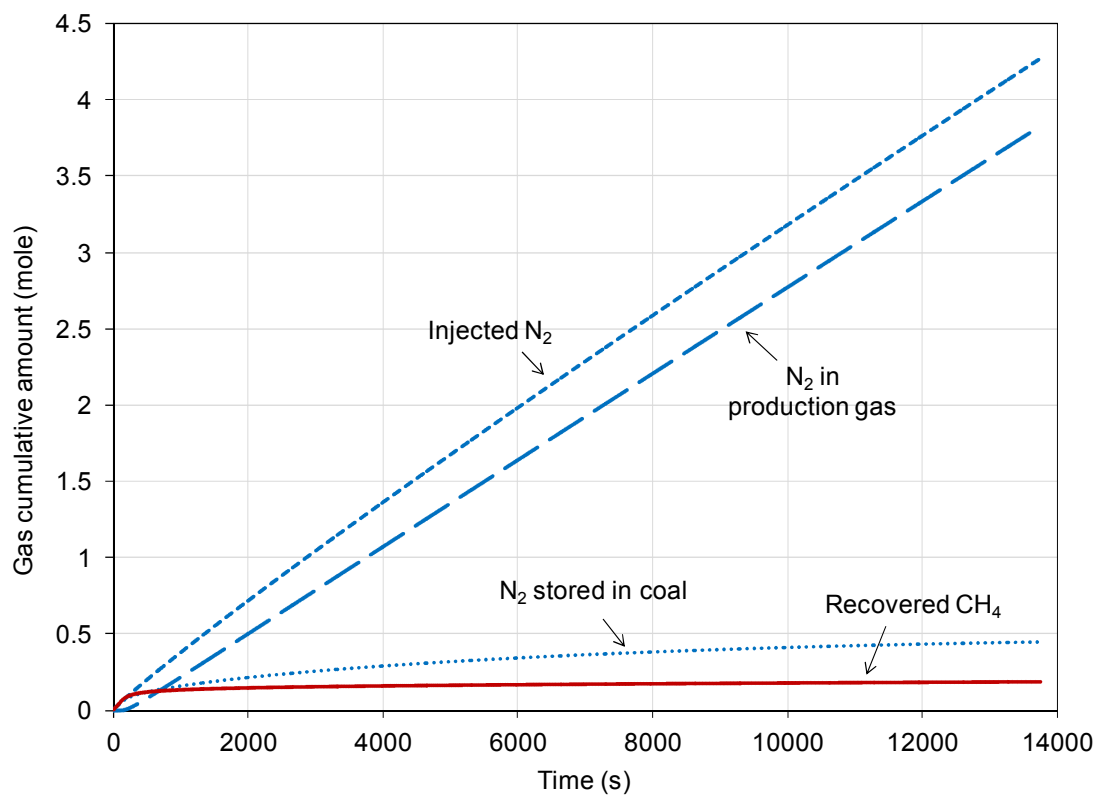


Figure 6. The composition of the production gas with time during the N<sub>2</sub> experiment.



**Figure 7.** The composition of the production gas with time during the CO<sub>2</sub> experiment.



**Figure 8.** Cumulative amounts of N<sub>2</sub> injected, recovered and stored with time during the N<sub>2</sub>-ECBM experiment.

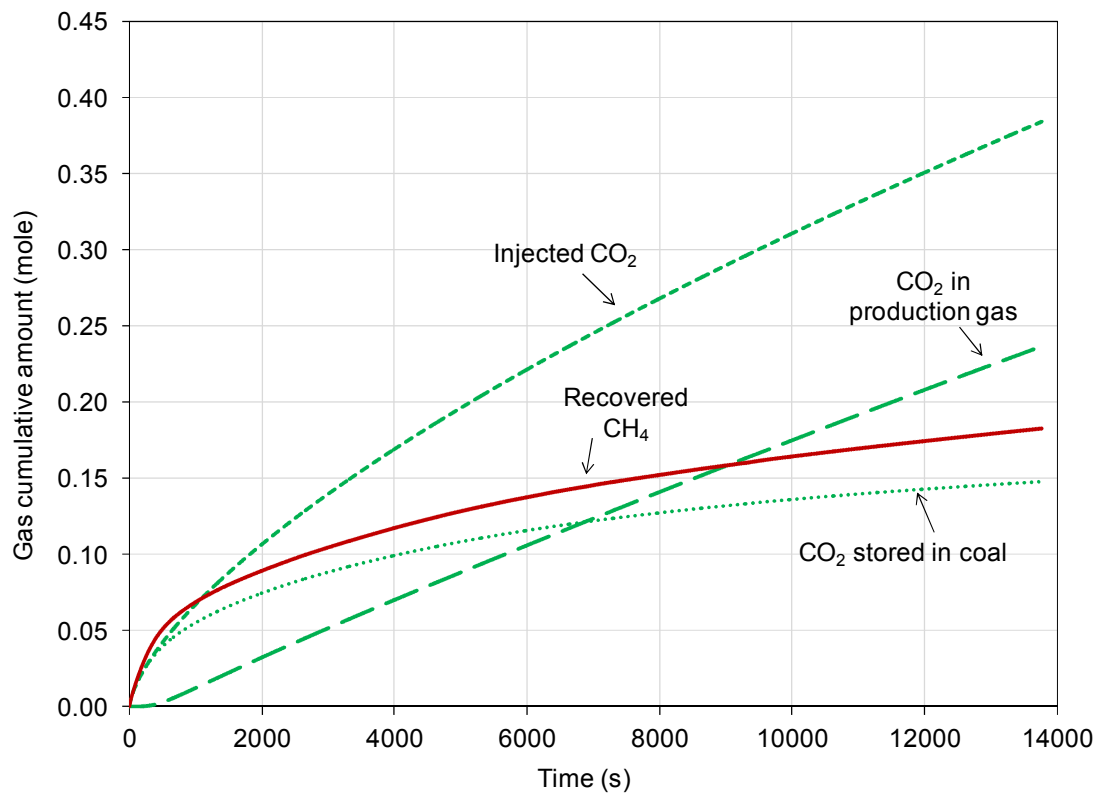


**Figure 9.** Cumulative amounts of CO<sub>2</sub> injected, recovered and stored with time during the CO<sub>2</sub>-ECBM experiments.



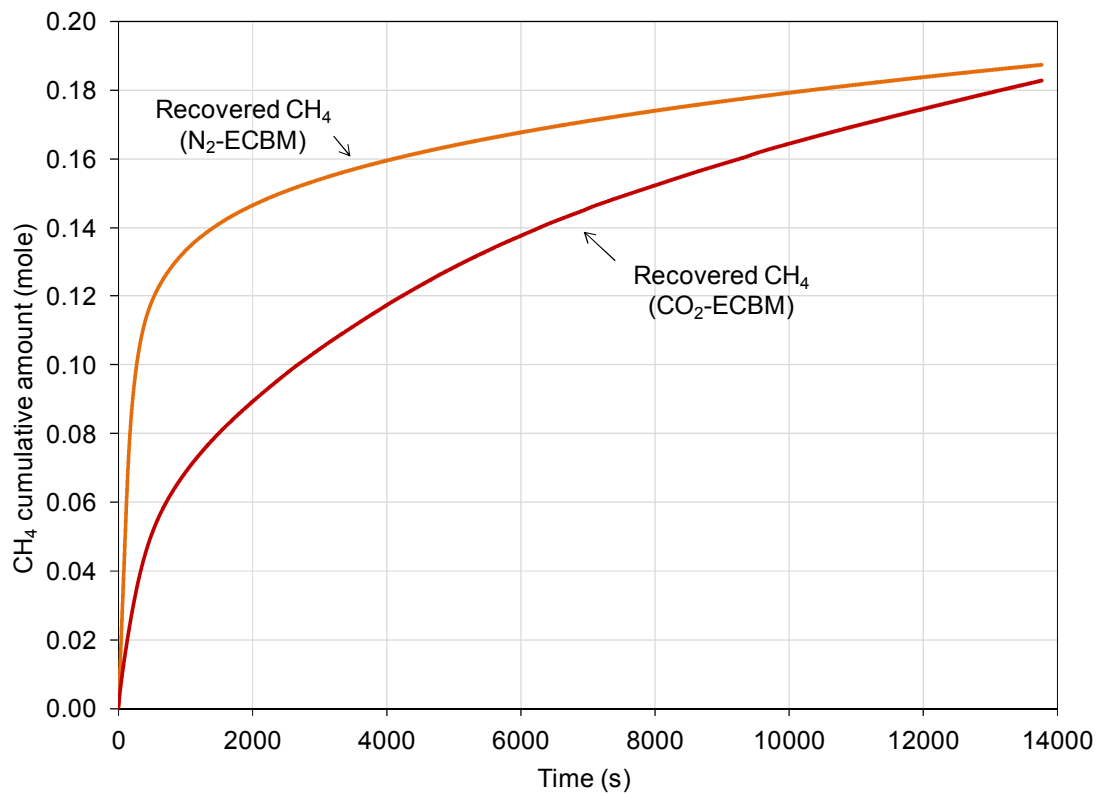


**Figure 10.** Cumulative amounts of CH<sub>4</sub> recovery during the N<sub>2</sub>-ECBM and CO<sub>2</sub>-ECBM experiments.

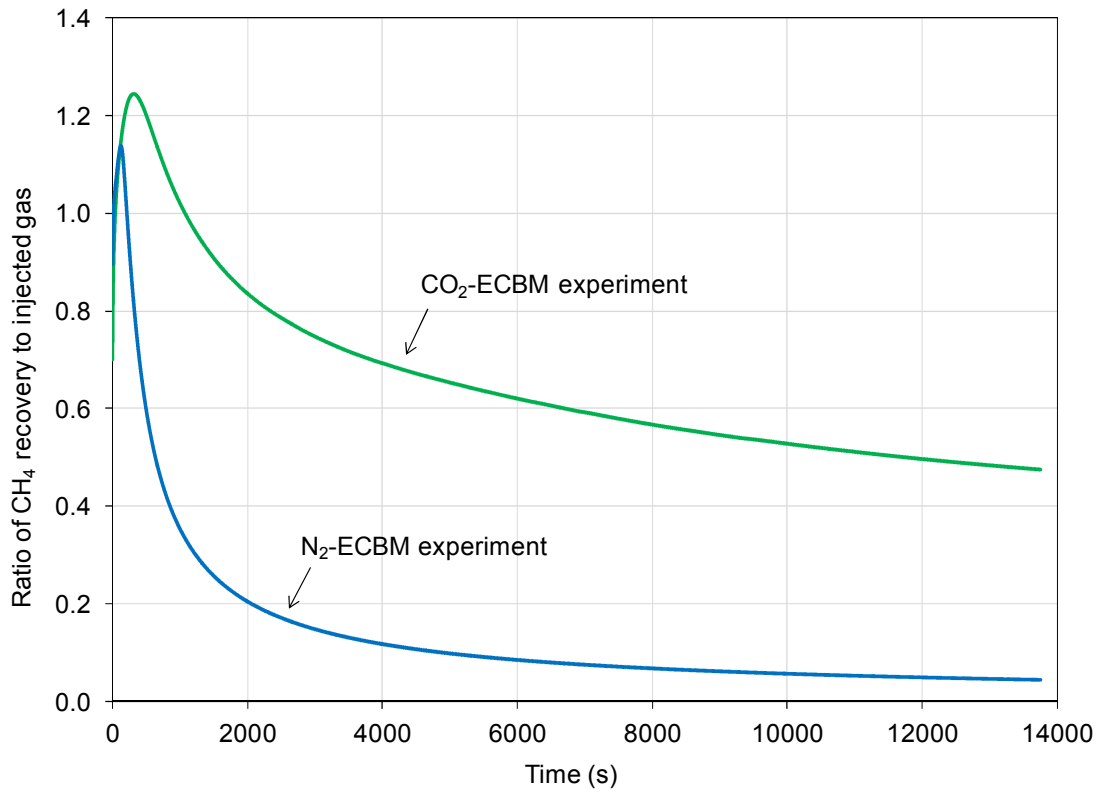


**Figure 11.** The ratio of CH<sub>4</sub> recovery to injected gas and its variation with time.

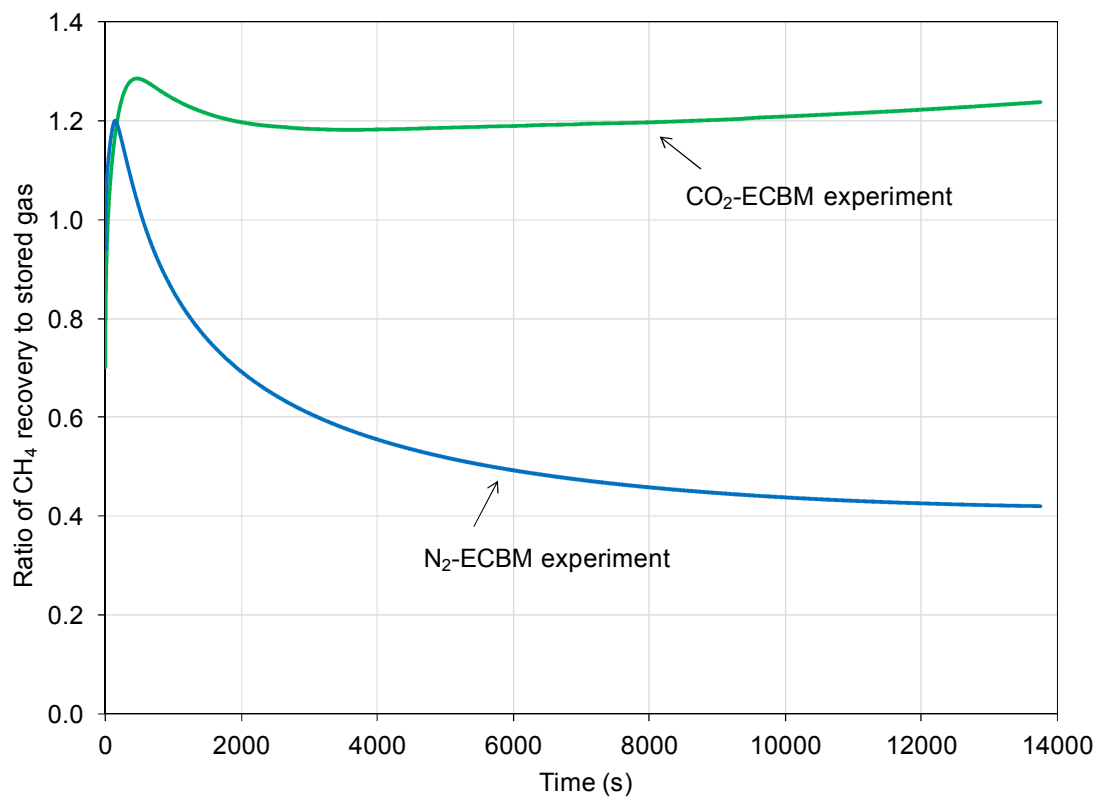


**Figure 12.** The ratio of CH<sub>4</sub> recovery to stored gas and its variation with time.